Analyst

Interdisciplinary detection science

www.rsc.org/analyst

Volume 135 | Number 4 | April 2010 | Pages 645–808

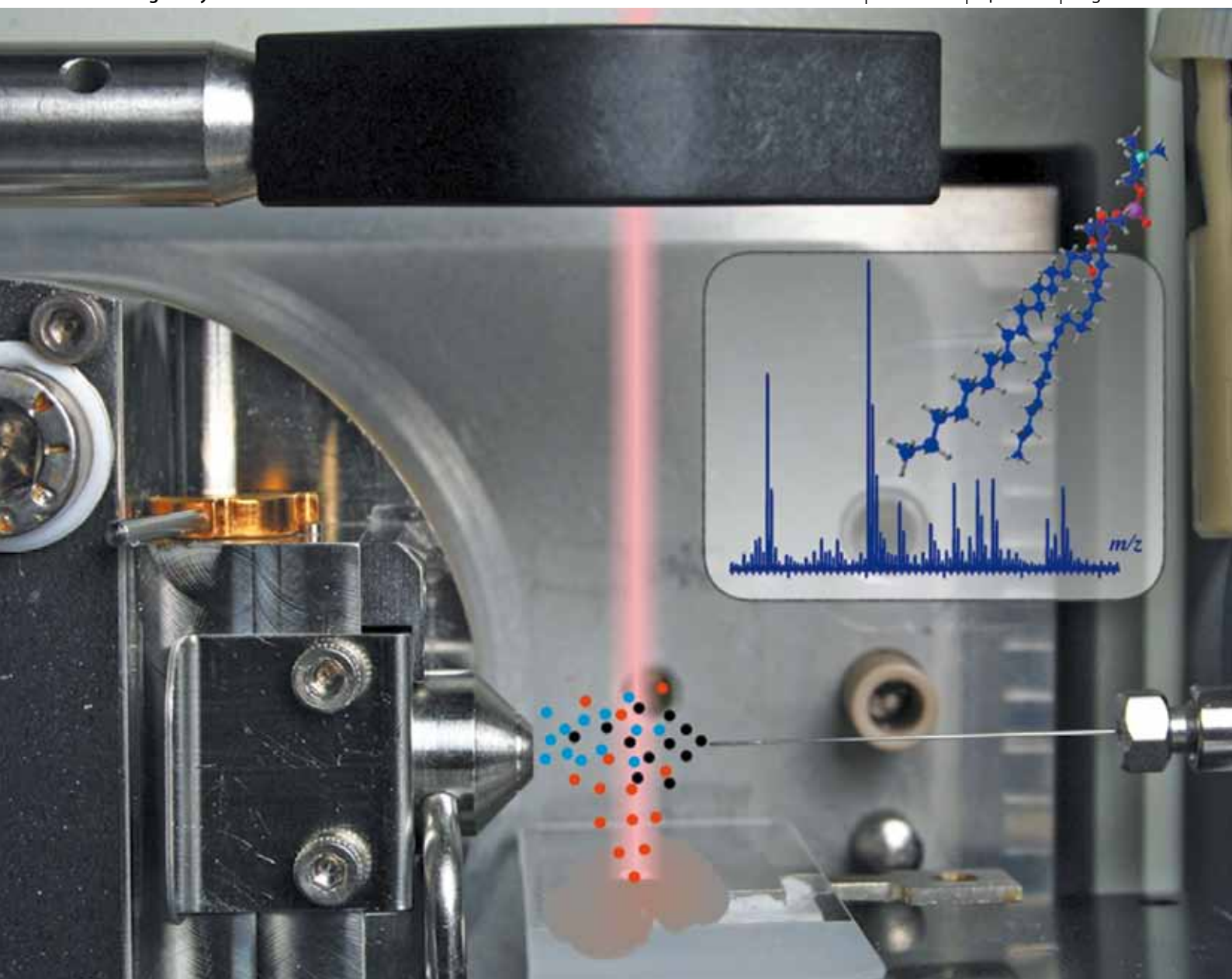

Themed Issue on Ambient Mass Spectrometry

ISSN 0003-2654

RSC Publishing

Direct analysis of lipids and small metabolites in mouse brain tissue by AP IR-MALDI and reactive LAESI mass spectrometry†‡

Bindesh Shrestha,[a] Peter Nemes,[a] Javad Nazarian,[b] Yetrib Hathout,[b] Eric P. Hoffman[b] and Akos Vertes*[a]

Received 2nd November 2009, Accepted 7th January 2010
First published as an Advance Article on the web 20th January 2010
DOI: 10.1039/b922854c

Ambient analysis of metabolites and lipids from unprocessed animal tissue by mass spectrometry remains a challenge. The utility of the two novel ambient ionization techniques – atmospheric pressure infrared matrix-assisted laser desorption ionization (AP IR-MALDI) and laser ablation electrospray ionization (LAESI) – is demonstrated for the direct mass spectrometric analysis of lipids and other metabolites from mouse brain. Major brain lipids including cholesterol, various phospholipid species (glycerophosphocholines, sphingomyelin and phosphatidylethanolamines) along with numerous metabolites, for example γ-aminobutyric acid (GABA), creatine and choline, were identified in a typical mass spectrum. In a new ionization modality of LAESI, termed reactive LAESI, in-plume reactions with a solute of choice (lithium sulfate) enhanced structure-specific fragmentation of lipid ions for improved molecular assignment in collision-activated dissociation experiments. In-plume processes in reactive LAESI provide additional structural information without contaminating the biological sample with the reactant.

Introduction

Lipidomics is broadly defined as the analysis of lipids and lipid-associated species. Apart from their structural role, lipids also act as signaling molecules or precursors to such molecules in the nervous system. As such, many neurological disorders such as schizophrenia and Alzheimer's disease are linked to abnormal lipid metabolism.[1–4] The mammalian brain is not only rich in lipid content but also contains a structurally diverse lipid population.[1] More than half of the dry weight of a normal human brain is composed of lipids, predominantly glycerophospholipids.[5,6] These species play vital roles such as the generation of second messengers, apoptosis, regulation of transporters and membrane-bound enzymes, and the maintenance of neuronal wellbeing.[7]

Imbalances in brain metabolites are responsible for many neurological diseases and neurocognitive conditions.[8,9] Since many small metabolites are directly or indirectly involved with lipid metabolism, their detection helps to gain a better understanding of lipid function. Currently the *in vivo* analysis of metabolites is achieved by microdialysis sampling[10] or by non-invasive measurements with nuclear magnetic resonance (NMR)[11,12] or positron emission tomography (PET)[13] that exhibit low sensitivity. Improved detection limits for brain neurotransmitters and metabolites can be achieved using mass spectrometric techniques, such as LC/MS,[14] CE-ESI-MS/MS[15] and LC/ESI MS/MS,[16] which require extensive sample preparation and long analysis time. Recently, the utility of atmospheric pressure photoionization and atmospheric pressure chemical ionization was demonstrated for neurotransmitters.[17]

Several techniques are available for the analysis of lipids *in vivo* and *in vitro*. Nuclear magnetic resonance (NMR) based on ^{31}P nuclei for phospholipids and protons for all other lipids has demonstrated excellent capabilities for the *in vivo* analysis of lipids.[18] Chromatographic techniques, such as thin layer chromatography (TLC),[19,20] high performance liquid chromatography (HPLC) and gas chromatography (GC), are often used for the analysis of extracted lipid samples.[21] Mass spectrometry (MS) is another powerful approach for the investigation of lipids,[22] for example, in combination with traditional ionization techniques such as secondary ion mass spectrometry (SIMS)[23] and fast atom bombardment (FAB).[24] Two soft ionization techniques, electrospray ionization (ESI)[25–27] and matrix-assisted laser desorption ionization (MALDI),[28–30] have been utilized to analyze lipids from processed biological samples. The direct analysis of lipids from brain tissue using vacuum or intermediate pressure MALDI requires the application of an external matrix and the transfer of the sample into the low-pressure environment.[31–36] Sample processing as well as the post-mortem cellular disintegration of autopsied biological samples require special care to maintain the molecular integrity of samples.[37,38] Clearly, technical developments are needed in the way sampling and molecular analysis is performed to mitigate such effects.

Novel MS-based approaches employing ambient ion sources present unique advantages for the investigation of biological samples, including brain sections. As these methods probe the

[a]*Department of Chemistry, W. M. Keck Institute for Proteomics Technology and Applications, George Washington University, Washington, DC 20052, USA. E-mail: vertes@gwu.edu; Fax: +1-202-994-5873; Tel: +1-202-994-2717*
[b]*Research Center for Genetic Medicine, Children's National Medical Center, Washington, DC 20010, USA*

† This paper is part of an *Analyst* themed issue on Ambient Mass Spectrometry, with guest editors Xinrong Zhang and Zheng Ouyang.

‡ Electronic supplementary information (ESI) available: tandem MS spectra of PC(18:1/18:1) lipid standard ions produced by LAESI and reactive LAESI. Tentative peak assignments of some ions in the AP IR-MALDI and LAESI mass spectra of normal mouse brain tissue. See DOI: 10.1039/b922854c

This journal is © The Royal Society of Chemistry 2010

molecular content of tissues under atmospheric-pressure conditions, they can help to minimize or eliminate artifacts linked to freeze–thawing and post-mortem tissue disintegration as well as provide the much desired capability of studying biological samples with minimal pretreatment. For example, desorption electrospray ionization (DESI) MS has already shown outstanding capabilities in assessing the chemical distribution in positive and negative ion mode of various lipids from brain and liver sections.[39–43] Similarly, electrospray-assisted laser desorption ionization (ELDI) MS has been utilized to characterize lipids in porcine brain tissue.[44]

At 2.94 μm wavelength, the strong absorption of the water molecules due to OH vibrations can be utilized to directly analyze tissue samples with a high water content including mammalian brains with *ca.* 80% water content.[45] Atmospheric pressure infrared matrix-assisted laser desorption ionization (AP IR-MALDI) MS, which directly samples ions generated by the infrared laser pulse, has been utilized to analyze metabolites and lipids from various plant organs and human bodily fluids.[46–48] Laser ablation electrospray ionization (LAESI) samples neutrals produced by the laser ablation followed by post-ionization by an electrospray. LAESI-MS has been employed for the analysis of metabolites from various plant organs, human bodily fluids, and the electric organ of the torpedo fish.[49–51] A technique similar to LAESI, IR matrix-assisted laser desorption electrospray ionization (MALDESI), was utilized to analyze carbohydrates and lipids in milk and egg yolk.[52] More recently, with the help of a sharpened optical fiber to reduce the focal spot size, we have demonstrated the capability of LAESI-MS to directly analyze metabolites from single plant and animal cells.[53]

In this contribution we demonstrate the utility of AP IR-MALDI and LAESI in the direct analysis of metabolites and lipids in mouse brain samples. To facilitate the structure elucidation of glycerophosphocholines (PC), we present a new variant of LAESI, termed reactive LAESI. Other reactive ambient ionization methods, reactive DESI and reactive ELDI[54–57] have demonstrated success in the analysis of antimalarial drugs, phosphonate hydrolysis, cholesterol, and proteins. In this approach, a reactant, *i.e.*, a lithium salt, is dissolved in the electrosprayed solution to produce droplets seeded with lithium ions. As the particulates from the laser ablation plume coalesce with the electrosprayed droplets, lithium adducts are produced from the molecules of the sample. For the lipid molecular class, the formation of lithiated ions is especially beneficial as these ions readily undergo structure-specific fragmentation enabling enhanced molecular assignments. The cationization of PC in reactive LAESI also reveals some mechanistic details of the interaction between the electrospray plume and the neutrals produced by the infrared laser ablation.

Experimental

Mass spectrometer and infrared laser

Positive ions generated by AP IR-MALDI and LAESI (see below) were detected by an orthogonal acceleration time-of-flight mass spectrometer (Q-TOF Premier; Waters Co., Milford, MA) with a custom-made interface described earlier (see Fig. 1).[46,49] The infrared 5 ns laser pulse at 2.94 μm wavelength

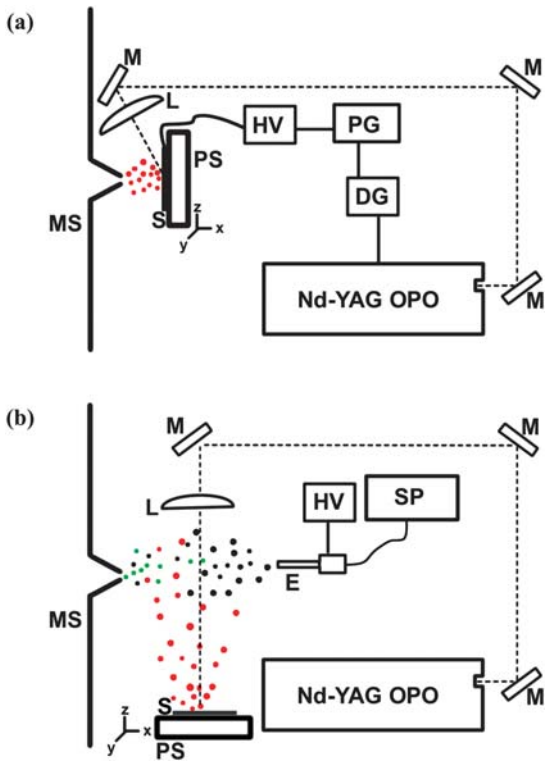

Fig. 1 Schematics of AP IR-MALDI and LAESI-MS. Pulses from the mid-IR Nd-YAG laser-driven OPO are focused onto the brain tissue sample (S) mounted on a Peltier stage (PS) using Au-coated mirrors (M) and a CaF_2 lens (L) and generate the ablation products (red dots). **(a)** In AP IR-MALDI, ions from the infrared ablation plume are directly extracted into the mass spectrometer (MS) with the help of a pulsed high voltage (HV) produced by a pulse generator (PG) and timed by a delay generator (DG). **(b)** In LAESI-MS, the neutrals in the ablation plume are intercepted by the electrospray plume (black dots) and post-ionized to form ions (green dots), which are sampled by the MS. The electrospray is created by applying a high voltage (HV) to the emitter (E) capillary at a constant flow rate controlled by a syringe pump (SP).

was generated by a Nd:YAG laser-driven optical parametric oscillator (OPO) (Vibrant IR; Opotek, Carlsbad, CA) running at a 10 Hz repetition rate. The laser beam was aligned by gold-coated mirrors (Thorlabs, Newton, NJ) and focused by a 50 mm focal length plano-convex calcium fluoride lens (Infrared Optical Products, Farmingdale, NY). Fragmentation of selected ions was achieved by collision-activated dissociation (CAD) in tandem MS experiments. The primary ions with typical collision energies between 15 and 50 eV were introduced into a collision cell filled with argon gas at 4×10^{-3} mbar pressure. The mass spectrometer was calibrated using standards for some lipid or metabolite species. The accurate *m*/*z* values were obtained from a mass spectrum averaged over 10 scans.

AP IR-MALDI MS

For improved ion collection efficiency, our home-built AP IR-MALDI interface used pulsed dynamic focusing[58] based on fast switching of a high voltage power supply (PS350; Stanford Research Systems, Sunnyvale, CA) from +3 kV to ground at

 This journal is © The Royal Society of Chemistry 2010

a particular delay time triggered by a digital delay generator (DG535; Stanford Research Systems).

The target plate was kept at a distance of 2 mm from the mass spectrometer orifice to maximize ion collection efficiency, while allowing access by the focused laser beam under a 45° angle. Although reducing this distance would increase the ion yield, further approaching the orifice with the sample at high voltage could induce an electrical breakdown. The laser fluence in the AP IR-MALDI experiments was 0.7 ± 0.1 J/cm^2.

LAESI-MS

The LAESI ion source has been described earlier.[49] Briefly, it is based on an electrospray setup with the emitter biased by a regulated high voltage power supply (PS350; Stanford Research Systems, Sunnyvale, CA). A methanol–water (1:1) mixture containing 0.1% (v/v) trifluoroacetic acid was pumped through a blunt tip emitter (130 μm i.d., 260 μm, o.d., model 90531; Hamilton Co., Reno, NV) by a syringe pump (Harvard 22; Harvard Apparatus, Holliston, MA) at a 2–5 μl/min flow rate and stable electrospray was maintained at 3000 V potential. The emitter was lined up with the orifice of the mass spectrometer and was located at a distance of 10–12 mm from it. The distance between the target and the emitter axis was varied between 10 and 15 mm. The laser beam, with 90° incidence angle, was focused on the target *ca.* 5 mm downstream from the emitter tip and delivered a fluence of 0.8 ± 0.1 J/cm^2.

Chemicals

Lipid standard samples were obtained from Avanti Polar Lipids Inc., Alabaster, AL. All other chemicals were purchased from Fisher Scientific (Boston, MA) and used without further purification. Lipid standards of various concentrations were prepared in 50% (v/v) MeOH solution by adding lipid stock solutions prepared in $CHCl_3$.

Mouse brain tissue

Mouse brain samples were obtained from a healthy C57Bl/10 mouse strain from the Jackson Laboratory (Bar Harbor, ME). The mice were euthanized by cervical dislocation at average ages of 12–14 months. All animal procedures and experiments complied fully with the principles set forth in the 'Guide for the Care and Use of Laboratory Animals' prepared by the Committee on Care and Use of Laboratory Animals of the Institute of Laboratory Resources, National Research Council, and were approved by the Children's National Medical Center's Institutional Animal Use and Care Committee. Their brain was immediately snap-frozen using isopentane cooled in liquid nitrogen and stored at −80 °C until the analysis. The brain was kept frozen on top of a block of dry ice covered with sheets of aluminium foil and sectioned while observing through a magnifying viewer. The samples were prepared by manually excising 400 μm thick transverse sections through the middle of the cerebrum with a sharp surgical scalpel. Brain sections were directly used for mass spectrometric analysis without any pretreatment.

Peltier cooling stage

Brain tissue kept at room temperature can undergo rapid biochemical changes and dehydration. To avoid such changes, the sections were kept just below the freezing temperature of the tissue at *ca.* −5 °C during the analysis by using a Peltier cooling stage.[59] The Peltier cooling stage was based on a ceramic thermoelectric module (Ferrotec Corp., Bedford, NH) attached by heat sink compound (GC Electronics, Rockford, IL) and glue (Henkel Loctite, Cleveland, OH) to a metal heat sink (Aavid Thermalloy, Concord, NH) and a DC fan (Comair Rotron, San Diego, CA). The thermoelectric module and the fan were powered by DC supplies (R.S.R. Electronics, Avenel, NJ).

Protocol for molecular assignments

Due to the large number of chemical species present in the biological tissue, the assignment of the detected ions required special attention. The tentative assignments of metabolites and lipids were obtained by a combination of accurate monoisotopic mass measurements, isotope distribution analysis, the use of metabolomic and lipid databases and, in some cases, CAD tandem MS. The theoretical monoisotopic masses were calculated using the NIST Isotope Calculator package (ISOFORM, Version 1.02). Metabolomic and lipid databases were searched for species within a ±15 mDa accuracy window of our mass spectrometric results. In particular, the detected molecules with low *m*/*z* were matched against known brain metabolites listed in the METLIN Metabolite Database[60] maintained by the Scripps Center for Mass Spectrometry (http://metlin.scripps.edu; last accessed on October 1, 2009) and in the Human Metabolome Database[61] maintained by Genome Alberta and Genome Canada (http://www.hmdb.ca; last accessed on October 1, 2009). The lipid databases included the LIPID Metabolites and Pathways Strategy resource maintained by the LIPID MAPS Consortium[62] (http://www.lipidmaps.org; last accessed on October 1, 2009), and the LipidBank[63] maintained by the Japanese Conference on the Biochemistry of Lipids (http://www.lipidbank.jp; last accessed on October 1, 2009). The results were reported following the comprehensive classification and nomenclature of lipids proposed by Fahy *et al*.[64] Even with extensive information, careful assignment of the metabolites and lipids is necessary due to the large number of possible structural isomers. An unambiguous identification of an ion needs comprehensive studies depending on multiple methods, such as separation techniques, ultrahigh resolution MS, NMR, FTIR, *etc*.

Results and discussion

AP IR-MALDI *vs.* LAESI-MS of a lipid standard

Initially, the production of lipid ions in AP IR-MALDI and LAESI experiments was assessed using a lipid standard. Fig. 2 presents the mass spectrum of the synthetic model lipid, PC(18:1/18:1), acquired by AP IR-MALDI and LAESI-MS. Comparison of the two spectra revealed that in AP IR-MALDI (see Fig. 2a) PC(18:1/18:1) underwent fragmentation losing, among others, the phosphocholine (PC) headgroup, whereas LAESI primarily produced the intact protonated molecular ion (see Fig. 2b). The other ions in the AP IR-MALDI spectrum might be due to

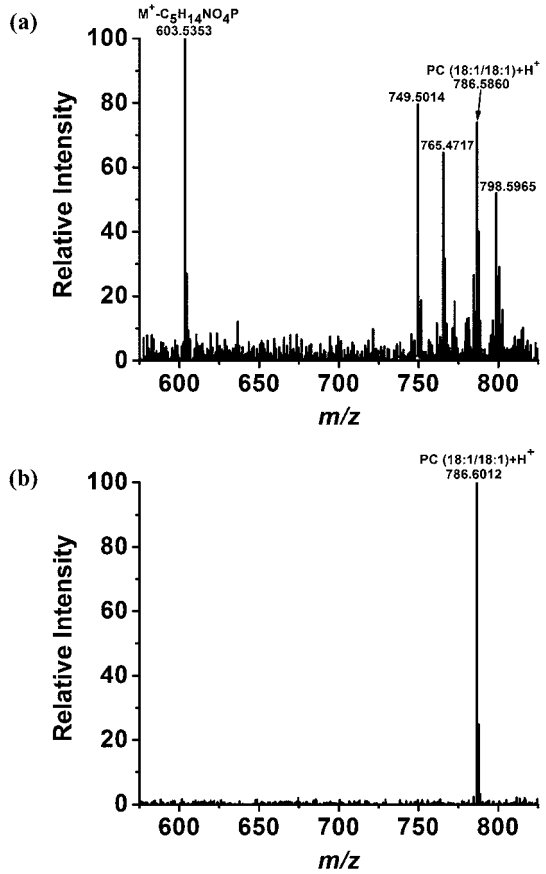

Fig. 2 Ambient mass spectra of PC(18:1/18:1) synthetic model lipid by **(a)** AP IR-MALDI and **(b)** LAESI indicate softer ion generation *via* the latter method.

fragmentation of the analyte or the presence of contamination. Recalling the sampling conditions for the two ionization modes helps to understand the differences between these spectra. While in AP IR-MALDI the primary laser ablation plume, produced by the phase explosion of the liquid, is sampled for ions,[65] in LAESI, the neutral particulate matter ejected by the recoil pressure is post-ionized by an electrospray source.[49] Thus, the lack of fragmentation observed in LAESI is consistent with the less energetic sample ejection process.

Analysis of brain metabolites

Direct AP IR-MALDI and LAESI analysis of mouse brain sections produced mass spectra dominated by small metabolites and phospholipids, such as PC (see Fig. 3 and 4, respectively). Detailed analysis of the spectra further revealed the presence of monoradylglycerols (MG), diradylglycerols (DG), phosphatidylethanolamines (PE), glycerophosphoglycerols (PG) and phosphosphingolipids (SM). Detailed lists of the metabolites and lipids detected by AP IR-MALDI and LAESI are provided in Tables S2 and S3, respectively, in the Electronic Supplementary Information.‡ Consistent with earlier reports that indicated predominant alkalination instead of protonation for MALDI at elevated pressures,[66–68] in AP IR-MALDI lipids were detected primarily as potassiated and sodiated molecules. In contrast,

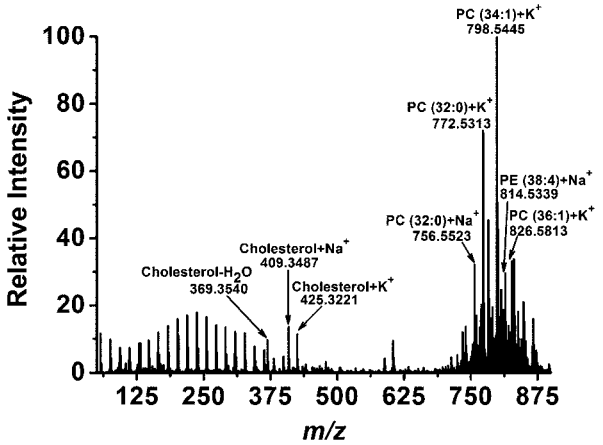

Fig. 3 Positive ion AP IR-MALDI mass spectrum from a transverse section of mouse brain cerebrum. Endogenous metabolite ions are observed in the m/z < 400 range. The spectrum was dominated by potassiated and sodiated phospholipids in the m/z > 700 range. The cholesterol was detected in its alkalinated form or after a water loss. The equidistant peak series in the low mass region corresponds to water clusters.

even though alkali cation concentrations were generally high in the brain tissue, the LAESI mass spectra were dominated by protonated peaks with sodiated ions present in only a few cases.

In addition to lipids, small brain metabolites were also present in both the AP IR-MALDI and the LAESI spectra (see Tables S2 and S3, respectively, in the Electronic Supplementary Information‡). Accurate mass measurements with sufficient mass resolution were needed to make the assignments for 44 small metabolites. For example, γ-aminobutyric acid (GABA), a major inhibitory neurotransmitter in the mammalian brain,[69] and choline, a precursor to many lipids and a neurotransmitter,[70] were both expected to be present with a nominal m/z of 104. The calculated accurate monoisotopic masses of the protonated GABA ion and the choline cation were only 36.3 mDa apart. The

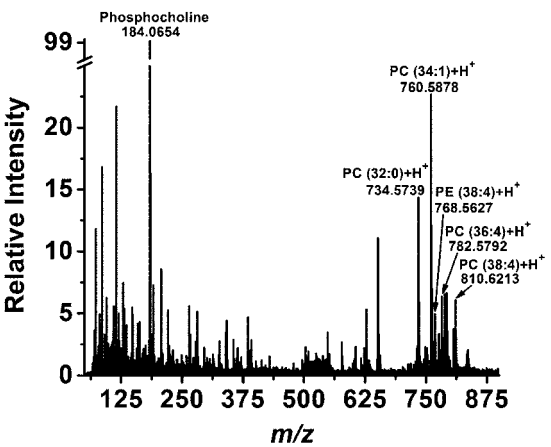

Fig. 4 Positive ion LAESI mass spectrum recorded from a transverse section of mouse brain cerebrum. Phosphocholine, at m/z 184.0654, also found in the polar headgroup of PCs, was the base peak in the spectrum. Endogenous metabolite ions from the brain were observed in the m/z < 400 range and the m/z > 700 region revealed the presence of various protonated phospholipids.

This journal is © The Royal Society of Chemistry 2010

corresponding peaks were close to baseline resolved by both AP IR-MALDI and LAESI. Mass accuracies for the ions identified in the mass spectra were uniformly below 15 mDa in the m/z < 900 mass range. Inspecting Tables S2 and S3 reveals that the two methods presented above offer complementary information for metabolite analysis directly from the brain tissue. Of the 143 overall assignments (79 for AP IR-MALDI and 93 for LAESI-MS), 29 are present in both spectra corresponding to a *ca.* 20% overlap. To account for the differences, we need to take into consideration that the samples are inhomogeneous and there are numerous unassigned peaks.

Cholesterol

The detection of cholesterol, one of the most abundant steroid lipids, by mass spectrometry is hindered by its inefficient ionization. In addition to being critical for the regulation of cell membrane properties in mammalian cells, cholesterol also acts as a precursor to other metabolites such as steroid hormones, bile acids and vitamin D.[71,72] Cholesterol was readily detected by AP IR-MALDI at m/z 369.3540, 409.3487 and 425.3221 as $[M - H_2O + H]^+$, $[M + Na]^+$ and $[M + K]^+$, respectively (see Fig. 3). In wet samples the alkaline adduct ions were more abundant. Interestingly, cholesterol spectra were also produced from dried samples with the $[M - H_2O + H]^+$ ion becoming more prominent. The ionization of cholesterol with AP IR-MALDI in the absence of water could be explained by the absorption of the O–H bond in the cholesterol molecule at 2.94 μm laser wavelength as shown in the condensed phase FTIR spectrum (see, for example, http://webbook.nist.gov/).

In the positive ion mode, relatively non-polar molecules, such as cholesterol, are poorly ionized by electrospray ionization. Thus usually derivatization, for example, to cholesterol-3-sulfate, is carried out to facilitate their detection.[73] In the LAESI spectrum of the mouse brain sample, the cholesterol ion could be detected only as a minor $[M - H_2O + H]^+$ peak after scanning a wider sample surface. However, the analysis of a wetted synthetic cholesterol sample by LAESI readily produced a peak at m/z 369.3482 indicating the presence of the $[M - H_2O + H]^+$ ion. The ionization of synthetic cholesterol showed that LAESI was capable of ionizing a compound that absorbed the mid-IR laser light, even though it could not be ionized directly by ESI. Further studies on the effect of laser wavelength, electrospray solution composition, negative ion modality, and ion source geometry are needed to assess the ability of LAESI to ionize such non-polar analytes.

Glycerophosphocholines (PC)

Ion production from PC is efficient due to the presence of the positively charged quaternary amine moiety in these molecules. The brain tissue mass spectra from both AP IR-MALDI and LAESI are dominated by PC ions. The analysis of a standard phospholipid mixture by conventional MALDI showed the suppression of other lipids by PC.[74] Most of the ions in the 700–900 m/z range represent PC species with a variety of fatty acid moieties. Four PCs in brain tissue samples, PC(32:0), PC(34:1), PC(36:1), and PC(38:4), with some of the related diradylglycerol (DG) ions appeared as major peaks in both the AP IR-MALDI and the LAESI mass spectra.

The DG structures can be independent species in the tissue, fragment ions, and/or natural degradation products of PC. Fragmentation of PC molecules has been reported under vacuum UV-MALDI conditions.[29] In AP IR-MALDI, based on the accurate mass measurement alone, the m/z 723.5016 ion can be viewed as a sodiated glycerophosphate PA(36:2) molecule, $[C_{39}H_{73}O_8P + Na^+]$ or a sodiated fragment of PC(34:1) formed by the loss of trimethylamine ($-N(CH_3)_3$, Δm 59.0735), $[C_{39}H_{73}O_8P + Na^+]$, as both of these species have the same elemental composition. Similarly in LAESI, the m/z 577.5279 ion can be derived as a protonated fragment of PC(34:1) due to the loss of the polar phosphocholine ($C_5H_{14}NO_4P$, Δm 183.0660) headgroup, $[C_{37}H_{68}O_4 + H^+]$, or it can be rationalized as a protonated DG structure, such as DG(34:1) with the same elemental composition after water loss. Ion production from the model lipid PC(18:1/18:1) with LAESI did not show any evidence of phosphocholine loss, whereas AP IR-MALDI produced a protonated fragment with the loss of phosphocholine, $[C_{39}H_{70}O_4 + H^+]$, resulting in an ion that was indistinguishable from the protonated DG(36:2) species after water loss. In Tables S2 and S3‡ we only listed the assignment for the detected ions that required the least amount of rearrangement, supported by the analysis of standards, and/or positive match in the related database. Due to the limited mass accuracy, in some cases even the elemental compositions could not be unambiguously discerned. For example, in the AP IR-MALDI spectra, m/z 810.6011 could be explained as a sodiated PC(36:1) and/or as a protonated PC(38:4) because the exact masses of these ions were only 2.3 mDa apart. Coupling AP IR-MALDI and LAESI with ultrahigh resolution MS should enable unambiguous identification in such cases.

Other lipids

Lipids from two other major categories, PE and SM, were detected by both AP IR-MALDI and LAESI. Protonated and alkalinated PE(38:4) and PE(40:6) structures were observed in AP IR-MALDI with no fragmentation (see Table S2 in the Electronic Supplementary Information‡). In LAESI, PE were detected as protonated molecules (see Table S3 in the Electronic Supplementary Information‡). Similar to the case of the PC assignments, these measured m/z values were consistent with potential fragmentation of other lipids. For example, in ESI, the loss of the phosphoethanolamine headgroup was used as a diagnostic tool for the detection of the PE.[75,76] Based on the accurate mass alone the produced ion could also be explained *via* a water loss from a DG. Other lipid assignments included a few instances of MG, glycerophosphates (PA), glycerophosphoglycerols (PG), SM and ceramide (Cer), implicated in the hydrolysis of SM. The ability to detect diverse lipids through AP IR-MALDI and LAESI-MS directly from the tissue can be used to uncover brain lipid profiles.

The mass spectra for standard samples were reproducible for both techniques. While most of the major peaks remained unchanged, for biological samples, due to their heterogeneity, the minor peaks showed some variance.

Structural elucidation by reactive LAESI

In light of the complexity of analogous lipid structures and the ambiguity of assignments based on the accurate mass alone, ion dissociation strategies were explored in combination with tandem MS. Conventional CAD of lipid molecular ions, however, often produces little additional information. For example, the CAD of the standard PC(18:1/18:1), at nominal *m/z* 787, produces a single fragment ion with *m/z* 184 indicating the presence of the phosphocholine headgroup but leaving the individual lengths of the acyl chains unexplored (see Fig. S1 in the Electronic Supplementary Information‡). Structure-specific fragmentation at the ester bonds is necessary to identify the acyl chain lengths and to narrow the set of potential lipid structures compatible with the *m/z* value.

Several MS-based methods, including MALDI, ESI, *etc.*, have noted that lithiated lipid molecules undergo extensive fragmentation by CAD that can enhance the identification of the fatty acyl chains.[77,78] In order to form the PC lithium adduct in AP IR-MALDI, it would be necessary to deposit the lithium salt onto the tissue, which might result in analyte redistribution in the sample. In contrast, LAESI enables the introduction of the lithiating agent through the electrospray process. Thus we added Li_2SO_4 to the electrospray solution in the LAESI source to produce lithiated ions from the ablated lipids. This new variant of LAESI, termed reactive LAESI provided an opportunity to introduce various reactions into the ion source.

To test the utility of reactive LAESI, CAD experiments were conducted on PC(18:1/18:1) with reactive LAESI ionization. The lithiated PC(18:1/18:1) generated by reactive LAESI with 500 μM Li_2SO_4 in the electrospray solution produced a variety of structure-specific fragments. This enabled the assignment of PC(18:1/18:1). See Fig. S2 in the Electronic Supplementary Information.‡

The reactive LAESI approach enabled us to elucidate the structure of several lipids that were detected directly in the mouse brain tissue. For example, the ion measured at *m/z* 766.5912 (see Fig. 5a) was subjected to CAD with 15–20 eV collision energy. As shown in Fig. 5b, the recorded tandem mass spectrum revealed neutral losses corresponding to palmitic acid (16:0), oleic acid (18:1), lithium palmitate, lithium oleate, and the combined losses of the fatty acids with trimethylamine (TMA), (16:0) + TMA and (18:1) + TMA. Based on this information the ion in question was identified as PC(16:0/18:1). In these experiments, the reactive LAESI methodology, in combination with CAD and tandem MS, gave additional insight into the structure of lipid ions produced directly from the tissue sample. Independent methodologies, including liquid chromatography and NMR can help to elucidate the location of the double bond in the (18:1) chain and the stereochemistry of the molecule.

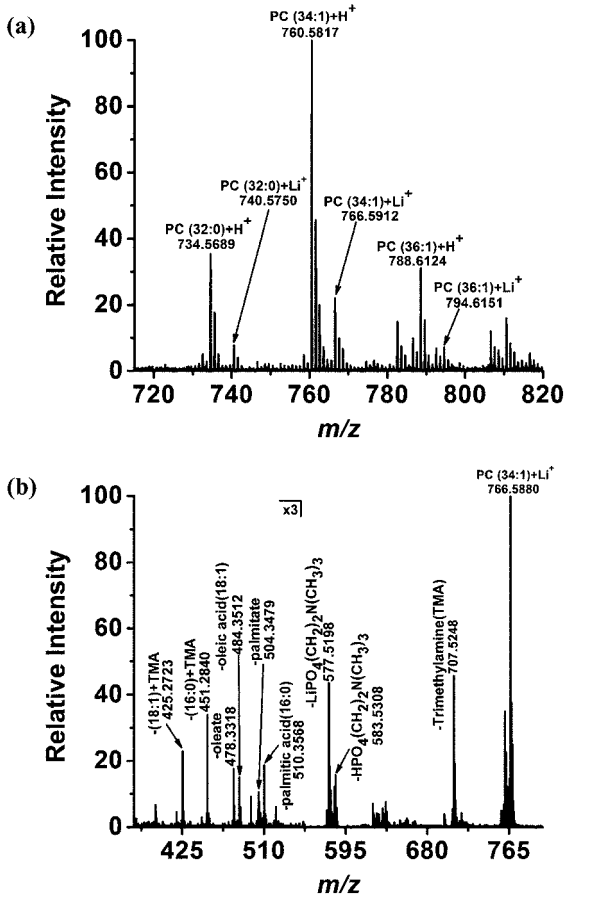

Fig. 5 Reactive LAESI experiments facilitated the structural elucidation of several lipid species. Some of the ablated lipid molecules were converted into lithium adducts upon coalescence with electrosprayed droplets seeded with Li^+ ions (see panel (a)). These lithiated lipid ions readily fragmented by CAD yielding fragments characteristic of the parent ion. For example, in panel (b), the ion measured at *m/z* 766.5912 produced fragment ions at *m/z* 707.5248, 583.5308, and 577.5198, corresponding to the loss of the trimethylamine [$N(CH_3)_3$, Δm 59.0735], phosphocholine [$C_5H_{14}NO_4P$, Δm 183.0660], and lithiated phosphocholine [$C_5H_{13}NO_4PLi$, $\Delta m/z$ 189.0742], respectively. Other fragment ions, including those registered at *m/z* 510.3568 and 484.3512 were formed through the neutral loss of palmitic acid (16:0) and oleic acid (18:1), respectively. This fragmentation pattern was consistent with the CAD fragmentation of the PC(16:0/18:1) + Li^+ lipid ion.

Relative quantitation of lipids in brain tissue

Earlier studies indicated that the ionization efficiency of phospholipid species by ESI MS depends on the length and the degree of saturation of its acyl chains, and most importantly on the structure of its headgroup.[26] To explore these potential disparities, LAESI mass spectra of the equimolar solution of PC(16:0), PE(18:1/16:0), PC(18:1/16:0), and PC(18:1/18:1) were recorded at 100 μM concentration for each of the components (see Fig. 6). The diacyl lipid ions with the same phosphocholine headgroup, PC(18:1/18:1) and PC(18:1/16:0), show similar ion counts in LAESI-MS, whereas diacyl lipid ions with the same acyl chains but different headgroups, PE(18:1/16:0) and PC(18:1/16:0), have significantly different ion counts.

The capability of quantitative analysis for small metabolites in *Torpedo californica* tissue by LAESI-MS had been demonstrated. The tissue was spiked with deuterium-labeled metabolites to aid quantitation. Similarly, to obtain concentration values for PC(34:1) in the mouse brain, spiking with deuterium-labeled PC(d-31)(34:1) was used at different concentrations. Then spiked tissue was ground in liquid nitrogen resulting in a homogenous paste.

This journal is © The Royal Society of Chemistry 2010

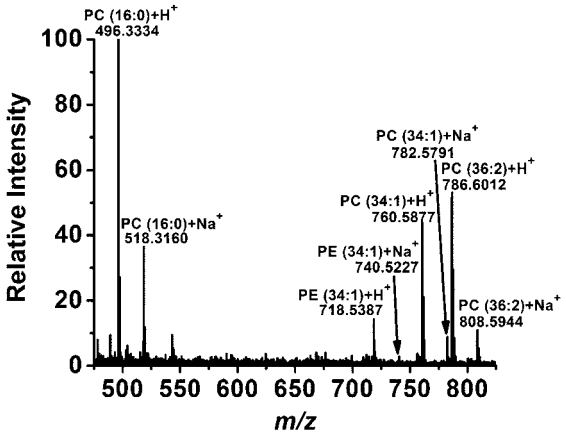

Fig. 6 LAESI mass spectra of a solution containing PC(16:0), PE(18:1/16:0), PC(18:1/16:0), and PC(18:1/18:1) at equimolar concentration shows that differences in glycerophospholipid ionization efficiencies depend on the structure of their headgroups and on the length and degree of saturation of their acyl chains.

The inset in Fig. 7 shows the typical LAESI spectrum of the ground tissue spiked with deuterated PC(d-31)(34:1). To quantitate PC(34:1), ion counts for the PC(d-31)(34:1) ion (*m*/*z* 790) and another ion, PC(32:0) at *m*/*z* 734, were measured. The ratio of ion counts for *m*/*z* 790/734 was plotted against the spiked concentration of PC(d-31)(34:1) as shown in Fig. 7. Linear regression produced a calibration curve with $R = 0.99$ correlation coefficient. Based on the regression, the concentration of PC(34:1) in the mouse brain was calculated to be 2.5×10^{-4} M.

Conclusions

Our results demonstrated the potential of AP IR-MALDI and LAESI for direct analysis of metabolites and lipids in neural tissues. The tentative assignment of more than 130 peaks, out of 206 detected ions, to more than 40 small metabolites and more than 45 species from diverse lipid classes (PC, MG, DG, PE, PG, SM and Cer) indicated the utility of these methods for applications in metabolomics. The ambient nature of the analysis also raised the prospect of studying physiological processes close to their native state, ultimately *ex vivo*, with minimal biochemical changes. Further development of this technique could lead to the identification of signaling molecules and their role in neurodegenerative diseases.

For lipid standards and in the analysis of brain tissue, reactive LAESI produced lithiated lipids that in CAD experiments readily fragmented at the ester bond. The produced structure-specific fragments enabled the determination of the acyl chain lengths and the number of double bonds within a chain. In order to achieve increased ion yields and desired fragmentation pathways, reactive LAESI can be extended by the use of a wide variety of reactants and/or surfactants in the electrospray solution. The modification of other experimental parameters, *e.g.*, electrospray polarity and solvents, and laser fluence, may help to detect other biomolecules, such as neuropeptides in the brain tissue.

MS-based chemical mapping techniques have already been used to investigate the effect of diseases on tissue composition. For example, UV-MALDI imaging indicated abnormal distribution of phospholipids in the liver metastasis of colon cancer, whereas DESI detected tumor boundaries in metastatic human liver adenocarcinoma.[39,79] Imaging by AP IR-MALDI can also be extended to brain and muscle tissue sections. LAESI-MS has recently shown success with molecular imaging of brain tissues.[80] Ambient spatial mapping of metabolites, lipids and, importantly, pharmaceuticals in animal tissues with IR laser ablation mass spectrometry holds the potential to enhance our understanding of metabolic response to diseases and the corrective action of drugs or drug candidates.

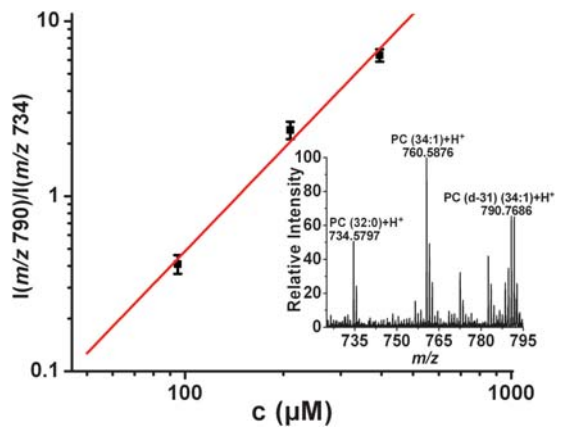

Fig. 7 Ion count ratio for deuterated PC(d-31)(34:1) and PC(32:0) expressed as $I(m/z\ 790)/I(m/z\ 734)$ *vs.* PC(d-31)(34:1) concentration in the mouse brain tissue. The inset shows the relevant part of the LAESI spectrum of the tissue spiked with PC(d-31)(34:1).

Acknowledgements

The authors recognize the financial support for this work from the National Science Foundation under grant 0719232, the W. M. Keck Foundation (041904), Protea Biosciences Inc., and the George Washington University Research Enhancement Fund. Any opinions, findings, and conclusions or recommendations expressed in this material are those of the authors and do not necessarily reflect the views of the supporting organizations. The PC(18:1/18:1) sample was kindly donated by Prof. Susan D. Gillmor of GWU.

References

1 P. S. Sastry, *Prog. Lipid Res.*, 1985, **24**, 69–176.
2 M. R. Wenk, *Nat. Rev. Drug Discovery*, 2005, **4**, 594–610.
3 E. Fahy, S. Subramaniam, H. A. Brown, C. K. Glass, A. H. Merrill, Jr., R. C. Murphy, C. R. H. Raetz, D. W. Russell, Y. Seyama, W. Shaw, T. Shimizu, F. Spener, G. van Meer, M. S. VanNieuwenhze, S. H. White, J. L. Witztum and E. A. Dennis, *J. Lipid Res.*, 2005, **46**, 839–862.
4 A. D. Watson, *J. Lipid Res.*, 2006, **47**, 2101–2111.
5 J. S. O'Brien and E. L. Sampson, *J. Lipid Res.*, 1965, **6**, 537–544.
6 R. M. Adibhatla, J. F. Hatcher and R. J. Dempsey, *AAPS J.*, 2006, **8**, E314–E321.
7 W. Dowhan, *Annu. Rev. Biochem.*, 1997, **66**, 199–232.
8 P. J. Hutchinson, M. T. O. Connell, P. J. Kirkpatrick and J. D. Pickard, *Physiol. Meas.*, 2002, **23**, R75.
9 I. K. Lyoo and P. F. Renshaw, *Biol. Psychiatry*, 2002, **51**, 195–207.
10 B. H. C. Westerink, *Behav. Brain Res.*, 1995, **70**, 103–124.
11 O. Henriksen, *NMR Biomed.*, 1995, **8**, 139–148.
12 J. F. A. Jansen, W. H. Backes, K. Nicolay and M. E. Kooi, *Radiology*, 2006, **240**, 318–332.

13 M. E. Phelps and J. C. Mazziotta, *Science*, 1985, **228**, 799–809.
14 S. Bourcier, J. F. Benoist, F. Clerc, O. Rigal, M. Taghi and Y. Hoppilliard, *Rapid Commun. Mass Spectrom.*, 2006, **20**, 1405–1421.
15 E. M. Jäverfalk-Hoyes, U. Bondesson, D. Westerlund and P. E. Andrén, *Electrophoresis*, 1999, **20**, 1527–1532.
16 E. Tareke, J. F. Bowyer and D. R. Doerge, *Rapid Commun. Mass Spectrom.*, 2007, **21**, 3898–3904.
17 T. J. Kauppila, T. Nikkola, R. A. Ketola and R. Kostiainen, *J. Mass Spectrom.*, 2006, **41**, 781–789.
18 M. Kriat, J. Vion-Dury, S. Confort-Gouny, R. Favre, P. Viout, M. Sciaky, H. Sari and P. J. Cozzone, *J. Lipid Res.*, 1993, **34**, 1009–1019.
19 I. R. Kupke and S. Zeugner, *J. Chromatogr., B: Biomed. Sci. Appl.*, 1978, **146**, 261–271.
20 J. C. Touchstone, *J. Chromatogr., B: Biomed. Sci. Appl.*, 1995, **671**, 169–195.
21 B. L. Peterson and B. S. Cummings, *Biomed. Chromatogr.*, 2006, **20**, 227–243.
22 R. C. Murphy, J. Fiedler and J. Hevko, *Chem. Rev.*, 2001, **101**, 479–526.
23 P. Sjovall, J. Lausmaa and B. Johansson, *Anal. Chem.*, 2004, **76**, 4271–4278.
24 N. Jensen, K. Tomer and M. Gross, *Lipids*, 1986, **21**, 580–588.
25 X. Han and R. W. Gross, *Proc. Natl. Acad. Sci. U. S. A.*, 1994, **91**, 10635–10639.
26 M. Pulfer and R. C. Murphy, *Mass Spectrom. Rev.*, 2003, **22**, 332–364.
27 X. Han and R. W. Gross, *Mass Spectrom. Rev.*, 2005, **24**, 367–412.
28 D. J. Harvey, *J. Mass Spectrom.*, 1995, **30**, 1333–1346.
29 J. A. Marto, F. M. White, S. Seldomridge and A. G. Marshall, *Anal. Chem.*, 1995, **67**, 3979–3984.
30 J. Schiller, R. Su, J. Arnhold, B. Fuchs, J. Leig, M. Muller, M. Petkovic, H. Spalteholz, O. Zschornig and K. Arnold, *Prog. Lipid Res.*, 2004, **43**, 449–488.
31 Y. Ishida, O. Nakanishi, S. Hirao, S. Tsuge, J. Urabe, T. Sekino, M. Nakanishi, T. Kimoto and H. Ohtani, *Anal. Chem.*, 2003, **75**, 4514–4518.
32 M. Rujoi, R. Estrada and M. C. Yappert, *Anal. Chem.*, 2004, **76**, 1657–1663.
33 S. N. Jackson, H. Y. J. Wang and A. S. Woods, *Anal. Chem.*, 2005, **77**, 4523–4527.
34 T. J. Garrett and R. A. Yost, *Anal. Chem.*, 2006, **78**, 2465–2469.
35 S. Cha and E. S. Yeung, *Anal. Chem.*, 2007, **79**, 2373–2385.
36 K. Dreisewerd, R. Lemaire, G. Pohlentz, M. Salzet, M. Wisztorski, S. Berkenkamp and I. Fournier, *Anal. Chem.*, 2007, **79**, 2463–2471.
37 T. L. Perry, S. Hansen and S. S. Gandham, *J. Neurochem.*, 1981, **36**, 406–412.
38 S. Banaschak, R. Rzanny, J. R. Reichenbach, W. A. Kaiser and A. Klein, *Int. J. Legal Med.*, 2005, **119**, 77–79.
39 J. M. Wiseman, S. M. Puolitaival, Z. Takáts, R. G. Cooks and R. M. Caprioli, *Angew. Chem., Int. Ed.*, 2005, **44**, 7094–7097.
40 J. M. Wiseman, D. R. Ifa, Q. Song and R. G. Cooks, *Angew. Chem., Int. Ed.*, 2006, **45**, 7188–7192.
41 N. E. Manicke, J. M. Wiseman, D. R. Ifa and R. G. Cooks, *J. Am. Soc. Mass Spectrom.*, 2008, **19**, 531–543.
42 Z. Takats, V. Kobliha, K. Sevcik, P. Novak, G. Kruppa, K. Lemr and V. Havlicek, *J. Mass Spectrom.*, 2008, **43**, 196–203.
43 A. L. Dill, D. R. Ifa, N. E. Manicke, Z. Ouyang and R. G. Cooks, *J. Chromatogr., B: Anal. Technol. Biomed. Life Sci.*, 2009, **877**, 2883–2889.
44 M.-Z. Huang, H.-J. Hsu, C. I. Wu, S.-Y. Lin, Y.-L. Ma, T.-L. Cheng and J. Shiea, *Rapid Commun. Mass Spectrom.*, 2007, **21**, 1767–1775.
45 L. L. Uzman and K. R. Marilynn, *J. Neurochem.*, 1958, **3**, 170–184.
46 Y. Li, B. Shrestha and A. Vertes, *Anal. Chem.*, 2007, **79**, 523–532.
47 Y. Li, B. Shrestha and A. Vertes, *Anal. Chem.*, 2008, **80**, 407–420.
48 B. Shrestha, Y. Li and A. Vertes, *Metabolomics*, 2008, **4**, 297–311.
49 P. Nemes and A. Vertes, *Anal. Chem.*, 2007, **79**, 8098–8106.
50 P. Nemes, A. A. Barton, Y. Li and A. Vertes, *Anal. Chem.*, 2008, **80**, 4575–4582.
51 P. Sripadi, J. Nazarian, Y. Hathout, E. P. Hoffman and A. Vertes, *Metabolomics*, 2009, **5**, 263–276.
52 J. S. Sampson, K. K. Murray and D. C. Muddiman, *J. Am. Soc. Mass Spectrom.*, 2009, **20**, 667–673.
53 B. Shrestha and A. Vertes, *Anal. Chem.*, 2009, **81**, 8265–8271.
54 L. Nyadong, M. D. Green, V. R. DeJesus, P. N. Newton and F. M. Fernandez, *Anal. Chem.*, 2007, **79**, 2150–2157.
55 Y. Song and R. G. Cooks, *J. Mass Spectrom.*, 2007, **42**, 1086–1092.
56 I. X. Peng, R. R. Ogorzalek Loo, J. Shiea and J. A. Loo, *Anal. Chem.*, 2008, **80**, 6995–7003.
57 C. Wu, D. R. Ifa, N. E. Manicke and R. G. Cooks, *Anal. Chem.*, 2009, **81**, 7618–7624.
58 P. V. Tan, V. V. Laiko and V. M. Doroshenko, *Anal. Chem.*, 2004, **76**, 2462–2469.
59 C. E. Von Seggern, B. D. Gardner and R. J. Cotter, *Anal. Chem.*, 2004, **76**, 5887–5893.
60 C. A. Smith, G. O'Maille, E. J. Want, C. Qin, S. A. Trauger, T. R. Brandon, D. E. Custodio, R. Abagyan and G. Siuzdak, *Ther. Drug Monit.*, 2005, **27**, 747.
61 D. S. Wishart, D. Tzur, C. Knox, R. Eisner, A. C. Guo, N. Young, D. Cheng, K. Jewell, D. Arndt, S. Sawhney, C. Fung, L. Nikolai, M. Lewis, M. A. Coutouly, I. Forsythe, P. Tang, S. Shrivastava, K. Jeroncic, P. Stothard, G. Amegbey, D. Block, D. D. Hau, J. Wagner, J. Miniaci, M. Clements, M. Gebremedhin, N. Guo, Y. Zhang, G. E. Duggan, G. D. MacInnis, A. M. Weljie, R. Dowlatabadi, F. Bamforth, D. Clive, R. Greiner, L. Li, T. Marrie, B. D. Sykes, H. J. Vogel and L. Querengesser, *Nucleic Acids Res.*, 2007, **35**, D521–D526.
62 D. Cotter, A. Maer, C. Guda, B. Saunders and S. Subramaniam, *Nucleic Acids Res.*, 2006, **34**, D507–D510.
63 K. Watanebe, E. Yasugi and M. Oshima, *Trends Glycosci. Glycotechnol.*, 2000, **12**, 175–184.
64 E. Fahy, S. Subramaniam, R. C. Murphy, M. Nishijima, C. R. H. Raetz, T. Shimizu, F. Spener, G. van Meer, M. J. O. Wakelam and E. A. Dennis, *J. Lipid Res.*, 2009, **50**, S9–14.
65 A. Vertes, P. Nemes, B. Shrestha, A. Barton, Z. Chen and Y. Li, *Appl. Phys. A: Mater. Sci. Proc.*, 2008.
66 P. B. O'Connor and C. E. Costello, *Rapid Commun. Mass Spectrom.*, 2001, **15**, 1862–1868.
67 T. J. Garrett, M. C. Prieto-Conaway, V. Kovtoun, H. Bui, N. Izgarian, G. Stafford and R. A. Yost, *Int. J. Mass Spectrom.*, 2007, **260**, 166–176.
68 A. Rohlfing, J. Muthing, G. Pohlentz, U. Distler, J. Peter-Katalinic, S. Berkenkamp and K. Dreisewerd, *Anal. Chem.*, 2007, **79**, 5793–5808.
69 M. Watanabe, K. Maemura, K. Kanbara, T. Tamayama and H. Hayasaki, *Int. Rev. Cytol.*, 2002, **213**, 1–47.
70 S. H. Zeisel, *J. Am. College Nutrit.*, 1992, **11**, 473–481.
71 K. Simons and E. Ikonen, *Science*, 2000, **290**, 1721–1726.
72 J. G. McDonald, B. M. Thompson, E. C. McCrum, D. W. Russell and H. A. Brown, *Methods in Enzymology*, Lipidomics and Bioactive Lipids: Mass-Spectrometry-based Lipid Analysis, Academic Press, 2007, vol. 432, pp. 145–170.
73 R. Sandhoff, B. Brugger, D. Jeckel, W. D. Lehmann and F. T. Wieland, *J. Lipid Res.*, 1999, **40**, 126–132.
74 M. Petkovic, J. Schiller, M. Muller, S. Benard, S. Reichl, K. Arnold and J. Arnhold, *Anal. Biochem.*, 2001, **289**, 202–216.
75 K. A. Zemski Berry and R. C. Murphy, *J. Am. Soc. Mass Spectrom.*, 2004, **15**, 1499–1508.
76 D. Schwudke, J. Oegema, L. Burton, E. Entchev, J. T. Hannich, C. S. Ejsing, T. Kurzchalia and A. Shevchenko, *Anal. Chem.*, 2006, **78**, 585–595.
77 F.-F. Hsu, A. Bohrer and J. Turk, *J. Am. Soc. Mass Spectrom.*, 1998, **9**, 516–526.
78 S. N. Jackson, H.-Y. J. Wang and A. S. Woods, *J. Am. Soc. Mass Spectrom.*, 2005, **16**, 2052–2056.
79 S. Shimma, Y. Sugiura, T. Hayasaka, Y. Hoshikawa, T. Noda and M. Setou, *J. Chromatogr., B: Anal. Technol. Biomed. Life Sci.*, 2007, **855**, 98–103.
80 P. Nemes, A. Svatos and A. Vertes, *57th American Society for Mass Spectrometry conference on Mass Spectrometry*, Philadelphia, PA, USA, 2009.

 This journal is © The Royal Society of Chemistry 2010

Electronic Supplementary Information (ESI) for Direct analysis of lipids and small metabolites in mouse brain tissue by AP IR-MALDI and reactive LAESI mass spectrometry

Bindesh Shrestha,[a] Peter Nemes,[b] Javad Nazarian,[b] Yetrib Hathout,[b] Eric P. Hoffman,[b] and Akos Vertes [*,a]

[a]*Department of Chemistry, W. M. Keck Institute for Proteomics Technology and Applications, George Washington University, Washington, DC 20052*
[b]*Research Center for Genetic Medicine, Children's National Medical Center, Washington, DC 20010*
** Corresponding author. Phone: +1(202)994-2717, Fax: +1(202)994-5873, Email: vertes@gwu.edu*

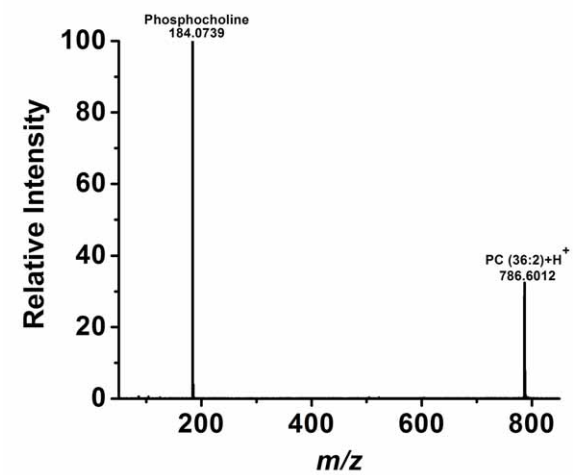

Figure S1. Tandem MS of the protonated PC(18:1/18:1) generated by LAESI produced a single fragment.

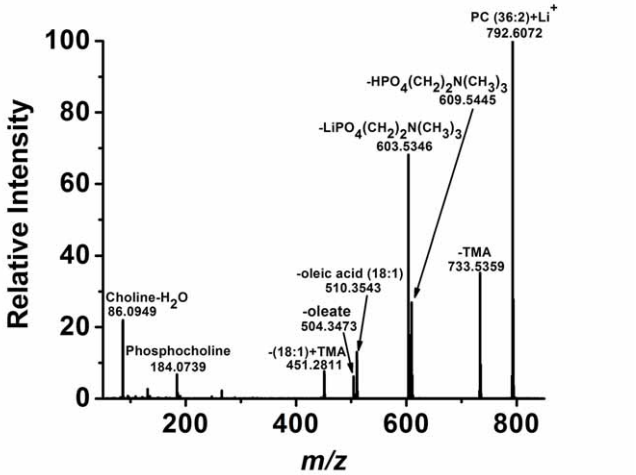

Figures S2. Tandem MS of the lithiated PC(18:1/18:1) generated by reactive LAESI produced structure-specific fragments.

LAESI vs. reactive LAESI tandem MS of DOPC

Except for the following modifications, all experimental conditions were the same as in the main section. In the LAESI experiments, a nanospray source was used. The source featured a tapered tip stainless steel emitter (i.d. 50 µm, MT320-50-5-5, New Objective, Woburn, MA), held at 2.8 kV high voltage. It sprayed methanol/water (1:1) mixture containing 0.1% (v/v) acetic acid at 200 nl/min flow rate. The mid-IR laser beam was focused with a 150 mm focal length CaF_2 lens (Infrared Optical Products, Farmingdale, NY). The >99% purity 1,2-dioleoyl-*sn*-glycero-3-phosphocholine (DOPC), corresponding to PC(18:1/18:1) in the LIPID MAPS nomenclature,[1] was obtained from Sigma Aldrich, St. Louis, MO, and used without further purification.

This model lipid was used to illustrate the utility of reactive LAESI for the determination of the acyl chain lengths and double bond counts in the PC. The CAD fragmentation of the protonated DOPC ion, at *m/z* 786.6012, produced a single fragment, the phosphocholine ion at *m/z* 184.0739 (see Figure S1). This showed the presence of the phosphocholine headgroup, sufficient to assign the compound as PC(36:2), but lacked any information on the length of the individual acyl chains and the distribution of double bonds. In reactive LAESI with 500 µM Li_2SO_4 in the electrospray solution, in addition to the protonated DOPC, the formation of lithiated DOPC at *m/z* 792.6072 was also observed. The tandem mass spectrum of the lithiated DOPC, obtained with CAD at 20-25 eV collision energy, showed the phosphocholine ion, and the ions due to the losses of trimethylamine (TMA), $HPO_4(CH_2)_2N(CH_3)_3$, $LiPO_4(CH_2)_2N(CH_3)_3$, oleic acid (18:1), oleate, and oleic acid + TMA from the lithiated molecule (Figure S2 and Table S1). The first four fragments indicated the presence of a phosphocholine headgroup and the last three fragments indicated the nature of the acyl chains. Thus, reactive LAESI using Li^+ as a reactant in combination with CAD revealed that the standard DOPC molecule indeed had a PC(18:1/18:1) structure.

Table S1. Mass accuracy of fragment ions produced by CAD of lithiated DOPC generated by reactive LAESI.

Fragment ions	Chemical formula[a]	m/z calc.	m/z meas.	△m (mDa)	ppm
PC(18:1/18:1) + Li^+	$C_{44}H_{84}NO_8PLi^+$	792.6094	792.6072	-2.2	-2.8
PC(18:1/18:1) – TMA + Li^+	$C_{41}H_{75}O_8PLi^+$	733.5359	733.5359	0	0.0
PC(18:1/18:1) – $HPO_4(CH_2)_2N(CH_3)_3$ + Li^+	$C_{39}H_{70}O_4Li^+$	609.5434	609.5445	1.1	1.8
PC(18:1/18:1) – Li $PO_4(CH_2)_2N(CH_3)_3$ + H^+	$C_{39}H_{71}O_4^+$	603.5353	603.5346	-0.7	-1.2
PC(18:1/18:1) – oleic acid + Li^+	$C_{26}H_{50}NO_6PLi^+$	510.3536	510.3543	0.7	1.4
PC(18:1/18:1) – oleate + H^+	$C_{26}H_{51}NO_6P^+$	504.3454	504.3473	1.9	3.8
PC(18:1/18:1) – (oleic acid + TMA) + Li^+	$C_{23}H_{41}O_6PLi^+$	451.2801	451.2811	1	2.2
phosphocholine	$C_5H_{15}NO_4P^+$	184.0739	184.0739	0	0.0
choline – H_2O	$C_5H_{12}N^+$	86.0970	86.0949	-2.1	-24.4

[a] The monoisotopic masses were calculated using the NIST Isotope Calculator package (ISOFORM, Version 1.02), and the measured *m/z* values were obtained from a typical mass spectrum.

Table S2. Tentative peak assignments for ions in the AP IR-MALDI mass spectrum of normal mouse brain tissue.

Metabolites and Lipids[a]	Chemical formula	Ion	m/z calc.	m/z meas.	Δm (mDa)	ppm
pyrrolidinone	C_4H_7NO	$M+H^+$	86.0606	86.0597	-0.9	-10.5
alanine	$C_3H_7NO_2$	$M+H^+$	90.0555	90.0551	-0.4	-4.4
γ-aminobutyric acid	$C_4H_9NO_2$	$M+H^+$	104.0712	104.0731	1.9	18.3
choline	$C_5H_{14}NO^+$	(+)	104.1075	104.1075	0	0.0
creatine	$C_4H_9N_3O_2$	$M+H^+$	132.0773	132.0775	0.2	1.5
hypoxanthine	$C_5H_4N_4O$	$M+H^+$	137.0463	137.0459	-0.4	-2.9
phosphoethanolamine	$C_2H_8NO_4P$	$M+H^+$	142.0269	142.0302	3.3	23.2
spermidine	$C_7H_{19}N_3$	$M+H^+$	146.1657	146.1690	3.3	22.6
imidazolone propionic acid	$C_6H_8N_2O_3$	$M+H^+$	157.0613	157.0642	2.9	18.5
dihydroorotate	$C_5H_6N_2O_4$	$M+H^+$	159.0406	159.0291	-11.5	-72.3
dihydroxymandelaldehyde	$C_8H_8O_4$	$M+H^+$	169.0501	169.0591	9	53.2
furoylglycine	$C_7H_7NO_4$	$M+H^+$	170.0453	170.0362	-9.1	-53.5
arginine	$C_6H_{14}N_4O_2$	$M+H^+$	175.1195	175.1199	0.4	2.3
methyltryptamine	$C_{11}H_{14}N_2$	$M+H^+$	175.1235	175.1199	-3.6	-20.6
hydroxytryptophan	$C_{11}H_{12}N_2O_3$	$M+H^+$	221.0926	221.0950	2.4	10.9
carnosine	$C_9H_{14}N_4O_3$	$M+H^+$	227.1144	227.1126	-1.8	-7.9
homocarnosine	$C_{10}H_{16}N_4O_3$	$M+H^+$	241.1301	241.1284	-1.7	-7.1
glycerophosphocholine	$C_8H_{20}NO_6P$	$M+H^+$	258.1106	258.1133	2.7	10.5
inosine	$C_{10}H_{12}N_4O_5$	$M+H^+$	269.0886	269.0917	3.1	11.5
		$M+K^+$	307.0445	307.0462	1.7	5.5
aminoimidazole ribonucleotide	$C_8H_{14}N_3O_7P$	$M+H^+$	296.0648	296.0662	1.4	4.7
arachidonic acid	$C_{20}H_{32}O_2$	$M+H^+$	305.2481	305.2340	-14.1	-46.2
cholesterol	$C_{27}H_{46}O$	$M-H_2O+H^+$	369.3521	369.3540	1.9	5.1
		$M+Na^+$	409.3446	409.3487	4.1	10.0
		$M+K^+$	425.3186	425.3221	3.5	8.2
N-arachidonoyl D-serine	$C_{23}H_{37}NO_4$	$M+H^+$	392.2801	392.2833	3.2	8.2
hydroxycholesterol	$C_{27}H_{46}O_2$	$M+K^+$	441.3135	441.3259	12.4	28.1
PC(O-16:1)	$C_{24}H_{50}NO_6P$	$M+K^+$	518.3013	518.3072	5.9	11.4
PC(16:0)	$C_{24}H_{50}NO_7P$	$M+K^+$	534.2962	534.3058	9.6	18.0
PC(20:4)	$C_{28}H_{50}NO_7P$	$M+H^+$	544.3403	544.3317	-8.6	-15.8
PC(18:1)	$C_{26}H_{52}NO_7P$	$M+Na^+$	544.3379	544.3317	-6.2	-11.4
Cer(d18:1/18:0)	$C_{36}H_{71}NO_3$	$M+Na^+$	588.5331	588.5372	4.1	7.0
		$M+K^+$	604.5071	604.5123	5.2	8.6
DG(34:1)	$C_{37}H_{70}O_5$	$M+Na^+$	617.5120	617.5239	11.9	19.3
DG(36:1)	$C_{39}H_{74}O_5$	$M+Na^+$	645.5433	645.5369	-6.4	-9.9
		$M+K^+$	661.5173	661.5209	3.6	5.4
DG(38:4)	$C_{41}H_{72}O_5$	$M+Na^+$	667.5277	667.5402	12.5	18.7
PA(34:1)	$C_{37}H_{71}O_8P$	$M+Na^+$	697.4784	697.4857	7.3	10.5
		$M+K^+$	713.4524	713.4602	7.8	10.9
PA(36:2)	$C_{39}H_{73}O_8P$	$M+Na^+$	723.4940	723.5016	7.6	10.5
		$M+K^+$	739.4680	739.4800	12	16.2
SM(18:0)	$C_{41}H_{84}N_2O_6P^+$	(+)	731.6067	731.6086	1.9	2.6
		$M-H+Na^+$	753.5886	753.5836	-5	-6.6
		$M-H+K^+$	769.5626	769.5598	-2.8	-3.6
PC(32:0)	$C_{40}H_{80}NO_8P$	$M+H^+$	734.5700	734.5776	7.6	10.3
		$M+Na^+$	756.5519	756.5523	0.4	0.5
		$M+K^+$	772.5258	772.5313	5.5	7.1
PC(34:1)	$C_{42}H_{82}NO_8P$	$M+H^+$	760.5856	760.5878	2.2	2.9
		$M+Na^+$	782.5675	782.5671	-0.4	-0.5
		$M+K^+$	798.5415	798.5445	3	3.8
PE(38:4)	$C_{43}H_{78}NO_8P$	$M+H^+$	768.5543	768.5493	-5	-6.5
		$M+Na^+$	790.5363	790.5342	-2.1	-2.7
PE(36:1)	$C_{41}H_{80}NO_8P$	$M+Na^+$	768.5519	768.5493	-2.6	-3.4
SM(24:0)	$C_{42}H_{84}NO_6P$	$M+K^+$	768.5673	768.5632	-4.1	-5.3

PC(36:4)	$C_{44}H_{80}NO_8P$	$M+H^+$	782.5700	782.5671	-2.9	-3.7
PC(O-34:1)	$C_{42}H_{84}NO_7P$	$M+K^+$	784.5622	784.5659	3.7	4.7
PS(36:2)	$C_{42}H_{78}NO_{10}P$	$M+H^+$	788.5441	788.5528	8.7	11.0
PC(O-36:5)	$C_{44}H_{80}NO_7P$	$M+Na^+$	788.5566	788.5528	-3.8	-4.8
PE(40:6)	$C_{45}H_{78}NO_8P$	$M+H^+$	792.5543	792.5460	-8.3	-10.5
PC(O-36:3)	$C_{44}H_{84}NO_7P$	$M+K^+$	808.5622	808.5589	-3.3	-4.1
		$M+Na^+$	814.5363	814.5339	-2.4	-2.9
		$M+K^+$	830.5101	830.5212	11.1	13.4
PG(36:0)	$C_{42}H_{83}O_{10}P$	$M+H^+$	801.5621	801.5630	0.9	1.1
		$M+Na^+$	817.5361	817.5458	9.7	11.9
PC(36:1)	$C_{44}H_{86}NO_8P$	$M+Na^+$	810.5989	810.6011	2.2	2.7
		$M+K^+$	826.5728	826.5813	8.5	10.3
PC(38:4)	$C_{46}H_{84}NO_8P$	$M+H^+$	810.6012	810.6011	-0.1	-0.1
		$M+Na^+$	832.5831	832.5697	-13.4	-16.1
PC(O-38:5)	$C_{46}H_{84}NO_7P$	$M+K^+$	832.5622	832.5697	7.5	9.0
PC(38:3)	$C_{46}H_{86}NO_8P$	$M+Na^+$	834.5989	834.5854	-13.5	-16.2
PC(O-38:4)	$C_{46}H_{86}NO_7P$	$M+K^+$	834.5779	834.5854	7.5	9.0
PC(38:6)	$C_{46}H_{80}NO_8P$	$M+Na^+$	828.5519	828.5660	14.1	17.0
		$M+K^+$	844.5258	844.5347	8.9	10.5
PS(36:0)	$C_{42}H_{82}NO_{10}P$	$M+K^+$	830.5313	830.5212	-10.1	-12.2
SM(24:1)	$C_{47}H_{94}N_2O_6P$	$M-H+K^+$	851.6408	851.6492	8.4	9.9
PC(40:6)	$C_{48}H_{84}NO_8P$	$M+Na^+$	856.5831	856.5961	13	15.2
		$M+K^+$	872.5571	872.5673	10.2	11.7
PC(40:1)	$C_{48}H_{94}NO_8P$	$M+Na^+$	866.6614	866.6537	-7.7	-8.9
PC(40:1)	$C_{48}H_{94}NO_8P$	$M+K^+$	882.6354	882.6407	5.3	6.0

[a]DG, PA, PC, PE, PS, PG, and SM species are identified by the total length of the acyl chain(s) and the number of double bonds in parentheses.

Table S3. Tentative peak assignments for ions in the LAESI mass spectrum of normal mouse brain tissue.

Metabolites and Lipids[a]	Chemical formula[c]	Ion	m/z calc.	m/z meas.	Δm (mDa)	ppm
pyrrolidine	C_4H_9N	$M+H^+$	72.0813	72.0835	2.2	30.5
aminoimidazole	$C_3H_5N_3$	$M+H^+$	84.0562	84.0470	-9.2	-109.5
ethanolamine	C_2H_7NO	$M+Na^+$	84.0425	84.0470	4.5	53.5
dehydroalanine	$C_3H_5NO_2$	$M+H^+$	88.0399	88.0458	5.9	67.0
γ-aminobutyric acid	$C_4H_9NO_2$	$M+H^+$	104.0712	104.0664	-4.8	-46.1
choline	$C_5H_{14}NO^+$	(+)	104.1075	104.1098	2.3	22.1
diaminopropionic acid	$C_3H_8N_2O_2$	$M+H^+$	105.0664	105.0714	5	47.6
diaminobutyric acid	$C_4H_{10}N_2O_2$	$M+H^+$	119.0821	119.0887	6.6	55.4
creatine	$C_4H_9N_3O_2$	$M+H^+$	132.0773	132.0828	5.5	41.6
hydroxyhexanoic acid	$C_6H_{12}O_3$	$M+H^+$	133.0865	133.0992	12.7	95.4
ornithine	$C_5H_{12}N_2O_2$	$M+H^+$	133.0977	133.0992	1.5	11.3
adenine	$C_5H_5N_5$	$M+H^+$	136.0623	136.0766	14.3	105.1
octenoic acid	$C_8H_{14}O_2$	$M+H^+$	143.1072	143.0955	-11.7	-81.8
spermidine	$C_7H_{19}N_3$	$M+H^+$	146.1657	146.1695	3.8	26.0
oxooctanoic acid	$C_8H_{14}O_3$	$M+H^+$	159.1021	159.1010	-1.1	-6.9
pyridoxamine	$C_8H_{12}N_2O_2$	$M+H^+$	169.0977	169.1058	8.1	47.9
furoylglycine	$C_7H_7NO_4$	$M+H^+$	170.0453	170.0464	1.1	6.5
arginine	$C_6H_{14}N_4O_2$	$M+H^+$	175.1195	175.1228	3.3	18.8
methyltryptamine	$C_{11}H_{14}N_2$	$M+H^+$	175.1235	175.1228	-0.7	-4.0
phosphoethanolamine	$C_2H_8NO_4P$	$M+K^+$	179.9828	179.9967	13.9	77.2
phosphocholine	$C_5H_{15}NO_4P^+$	(+)	184.0739	184.0665	-7.4	-40.2
metanephrine	$C_{10}H_{15}NO_3$	$M+H^+$	198.1130	198.1074	-5.6	-28.3
decenedioic acid	$C_{10}H_{16}O_4$	$M+H^+$	201.1127	201.1186	5.9	29.3
spermine	$C_{10}H_{26}N_4$	$M+H^+$	203.2236	203.2302	6.6	32.5
hydroxytryptophan	$C_{11}H_{12}N_2O_3$	$M+H^+$	221.0926	221.0905	-2.1	-9.5
acetylspermidine	$C_9H_{21}N_3O$	$M+K^+$	226.1322	226.1362	4	17.7
carnosine	$C_9H_{14}N_4O_3$	$M+H^+$	227.1144	227.1110	-3.4	-15.0
oxo-heneicosanoic acid	$C_{21}H_{40}O_3$	$M+H^+$	341.3056	341.3123	6.7	19.6
MG(18:0)	$C_{21}H_{42}O_4$	$M-H_2O+H^+$	341.3056	341.3123	6.7	19.6
methyl-eicosanoic acid	$C_{21}H_{42}O_2$	$M+K^+$	365.2822	365.2884	6.2	17.0
docosahexaenoic acid (DHA)	$C_{22}H_{32}O_3$	$M+K^+$	383.1989	383.1981	-0.8	-2.1
MG(22:6)	$C_{25}H_{38}O_4$	$M-H_2O+H^+$	385.2743	385.2793	5	13.0
FA(22:0)	$C_{22}H_{44}O_5$	$M+H^+$	389.3267	389.3127	14	-36.0
MG(22:4)	$C_{25}H_{42}O_4$	$M-H_2O+H^+$	389.3056	389.3127	7.1	18.2
N-palmitoyl dopamine (PALDA)	$C_{24}H_{41}NO_3$	$M+H^+$	392.3165	392.3029	-13.6	-34.7
dihydro PGF-1alpha	$C_{20}H_{38}O_5$	$M+K^+$	397.2356	397.2298	-5.8	-14.6
PC(16:0)	$C_{24}H_{50}NO_7P$	$M+H^+$	496.3403	496.3457	5.4	10.9
DG(O-32:2)	$C_{35}H_{66}O_4$	$M+H^+$	551.5039	551.5150	11.1	20.1
DG(34:1)	$C_{37}H_{70}O_5$	$M-H_2O+H^+$	577.5196	577.5279	8.3	14.4
		$M-H_2O+Na^+$	599.5015	599.5099	8.4	14.0
DG(36:4)	$C_{39}H_{68}O_5$	$M-H_2O+H^+$	599.5040	599.5099	5.9	9.8
DG(36:1)	$C_{39}H_{74}O_5$	$M-H_2O+H^+$	605.5509	605.5587	7.8	12.9
		$M-H_2O+Na^+$	627.5328	627.5398	7	11.2
DG(38:6)	$C_{41}H_{68}O_5$	$M-H_2O+H^+$	623.5040	623.5137	9.7	15.6
DG(38:5)	$C_{41}H_{70}O_5$	$M-H_2O+H^+$	625.5196	625.5303	10.7	17.1
DG(O-36:4)	$C_{39}H_{70}O_4$	$M+Na^+$	625.5172	625.5303	13.1	20.9
DG(38:4)	$C_{41}H_{72}O_5$	$M-H_2O+H^+$	627.5353	627.5398	4.5	7.2
PC(26:0)	$C_{34}H_{68}NO_8P$	$M+H^+$	650.4761	650.4668	-9.3	-14.3
PA(36:4)	$C_{39}H_{69}O_8P$	$M+H^+$	697.4808	697.4922	11.4	16.3
PA(34:1)	$C_{37}H_{71}O_8P$	$M+Na^+$	697.4784	697.4922	13.8	19.8
		$M+K^+$	713.4524	713.4468	-5.6	-7.8
PE(O-36:5)	$C_{41}H_{76}NO_7P$	$M+H^+$	724.5281	724.5334	5.3	7.3
PE(O-34:0)	$C_{39}H_{80}NO_7P$	$M+Na^+$	728.5570	728.5477	-9.3	-12.8
SM(24:0)	$C_{42}H_{84}NO_6P$	$M+H^+$	730.6114	730.5981	-13.3	-18.2
		$M+K^+$	768.5673	768.5632	-4.1	-5.3

SM(18:0)	$C_{41}H_{84}N_2O_6P^+$	(+)	731.6067	731.6075	0.8	1.1
PC(32:0)	$C_{40}H_{80}NO_8P$	$M+H^+$	734.5700	734.5739	3.9	5.3
		$M+K^+$	772.5258	772.5371	11.3	14.6
PA(36:2)	$C_{39}H_{73}O_8P$	$M+K^+$	739.4680	739.4753	7.3	9.9
PE(O-34:0)	$C_{39}H_{80}NO_7P$	$M+K^+$	744.5309	744.5372	6.3	8.5
PE(36:1)	$C_{41}H_{80}NO_8P$	$M+H^+$	746.5700	746.5798	9.8	13.1
		$M+Na^+$	768.5519	768.5632	11.3	14.7
PE(O-38:7)	$C_{43}H_{74}NO_7P$	$M+H^+$	748.5281	748.5361	8	10.7
PE(O-36:4)	$C_{41}H_{76}NO_7P$	$M+Na^+$	748.5257	748.5361	10.4	13.9
PE(O-38:5)	$C_{43}H_{78}NO_7P$	$M+H^+$	752.5594	752.5632	3.8	5.0
		$M+Na^+$	774.5413	774.5345	-6.8	-8.8
PE(O-36:2)	$C_{41}H_{80}NO_7P$	M+Na+	752.5570	752.5632	6.2	8.2
PC(34:1)	$C_{42}H_{82}NO_8P$	$M+H^+$	760.5856	760.5885	2.9	3.8
		$M+Na^+$	782.5675	782.5789	11.4	14.6
		$M+K^+$	798.5415	798.5381	-3.4	-4.3
PE(38:4)	$C_{43}H_{78}NO_8P$	$M+H^+$	768.5543	768.5632	8.9	11.6
PE(O-40:6)	$C_{45}H_{78}NO_7P$	$M+H^+$	776.5594	776.5668	7.4	9.5
PC(36:4)	$C_{44}H_{80}NO_8P$	$M+H^+$	782.5700	782.5789	8.9	11.4
PC(36:2)	$C_{44}H_{84}NO_8P$	$M+H^+$	786.6012	786.5970	-4.2	-5.3
		$M+Na^+$	808.5831	808.5852	2.1	2.6
PC(36:1)	$C_{44}H_{86}NO_8P$	$M+H^+$	788.6169	788.6199	3	3.8
		$M+Na^+$	810.5989	810.6104	11.5	14.2
PS(36:0)	$C_{42}H_{82}NO_{10}P$	$M+H^+$	792.5754	792.5665	-8.9	-11.2
PE(40:6)	$C_{45}H_{78}NO_8P$	$M+H^+$	792.5543	792.5665	12.2	15.4
PC(O-36:1)	$C_{44}H_{88}NO_7P$	$M+Na^+$	796.6196	796.6061	-13.5	-16.9
PC(O-36:2)	$C_{44}H_{88}NO_6P$	$M+K^+$	796.5986	796.6061	7.5	9.4
[glycan]Cer(d18:0/20:0)	$C_{44}H_{87}NO_8$	$M+K^+$	796.6068	796.6061	-0.7	-0.9
PC(38:6)	$C_{46}H_{80}NO_8P$	$M+H^+$	806.5700	806.5676	-2.4	-3.0
PC(36:3)	$C_{44}H_{82}NO_8P$	$M+Na^+$	806.5675	806.5676	0.1	0.1
PC(38:5)	$C_{46}H_{82}NO_8P$	$M+H^+$	808.5856	808.5852	-0.4	-0.5
PC(36:3)	$C_{44}H_{84}NO_8P$	$M+Na^+$	808.5831	808.5852	2.1	2.6
PC(38:4)	$C_{46}H_{84}NO_8P$	$M+H^+$	810.6012	810.6104	9.2	11.3
		$M+Na^+$	832.5831	832.5750	-8.1	-9.7
PC(40:7)	$C_{48}H_{82}NO_8P$	$M+H^+$	832.5856	832.5750	-10.6	-12.7
PC(O-38:5)	$C_{46}H_{84}NO_7P$	$M+K^+$	832.5622	832.5750	12.8	15.4
PC(40:6)	$C_{48}H_{84}NO_8P$	$M+H^+$	834.6012	834.6118	10.6	12.7
PC(38:3)	$C_{46}H_{86}NO_8P$	$M+Na^+$	834.5989	834.6118	12.9	15.5

[a]DG, PA, PC, PE, PS, PG, and SM species are identified by the total length of the acyl chain(s) and the number of double bonds in parentheses.

Reference:

1. E. Fahy, S. Subramaniam, R. C. Murphy, M. Nishijima, C. R. H. Raetz, T. Shimizu, F. Spener, G. van Meer, M. J. O. Wakelam and E. A. Dennis, *J. Lipid Res.*, 2009, **50**, S9-14.